Chaotic Modeling and Simulation (CMSIM) 4: 441–454, 2018

Stochastic vacuum: a new perspective on the "ether-drift" experiments

Maurizio Consoli[1]

INFN Sezione di Catania, Italy
(E-mail: maurizio.consoli@ct.infn.it)

Abstract. Basic foundational aspects of both quantum physics and relativity indicate that, at some fundamental level, the physical vacuum might behave as a stochastic medium, somehow similar to a highly turbulent ether. This picture, if taken seriously, might have phenomenological implications for the "ether-drift" experiments (from Michelson-Morley until the modern ones with optical resonators). Indeed, if there were a preferred reference frame, e.g. the system where the Cosmic Microwave Background (CMB) is exactly isotropic, the microscopic velocity field, which determines light anisotropy at the laboratory level, may differ sizeably from the macroscopic velocity field, as directly fixed by the earth cosmic motion. This would produce deviations from a standard Fourier analysis of the data and make it difficult to separate a genuine physical signal from spurious instrumental noise. With these premises, we have considered a theoretical framework where all measurable effects vanish exactly when light propagates in an "ideal" vacuum and where, within the analogy of a turbulent flow, there are random fluctuations of the local drift around the average earth motion. In this scheme, it is highly non trivial to understand if the irregular signal observed in present experiments with vacuum optical resonators is just spurious noise or has a genuine physical origin. We have thus compared with the classical experiments where light was still propagating in gaseous systems (air or helium at atmospheric pressure). In this case, the small irregular residuals observed in the various experiments become consistent with the same earth velocity of 370 km/s indicated by the direct CMB observations with satellites in space. In view of the substantial implications, for both physics and the history of science, new dedicated experiments and new methods of analysis are needed for a definite clarification.
Keywords: Michelson-Morley Experiments; Cosmic Microwave Background; Stochastic Vacuum.

1 Introduction

In 1887 Michelson and Morley tried to detect in laboratory a small difference of the velocity of light propagating in different directions that, according to classical physics, should have revealed the motion of the earth in the ether ("ether drift"). The result of their measurements, however, was much smaller than the classical prediction and considered as a typical instrumental artifact:

Received: 10 Jumy 2018 / Accepted: 24 October 2018

ISSN 2241-0503

a "null result". This was crucial to stimulate the first, pioneering formulations of the relativistic effects and, as such, represents a fundamental step in the history of science.

Nowadays, this original experiment and its early repetitions performed at the turn of 19th and 20th centuries (by Miller, Kennedy, Illingworth, Joos...) are considered as a venerable, well understood historical chapter for which, at least from a physical point of view, there is nothing more to refine or clarify. All emphasis is now on the modern versions of these experiments, with lasers stabilized by optical cavities that, apparently, have confirmed the null result by improving by many orders of magnitude on the limits placed by those original measurements.

Though, this is not necessarily true. In the original measurements, light was propagating in gaseous systems (air or helium at atmospheric pressure) while now, in modern experiments, light propagates in a high vacuum or inside solid dielectrics. Therefore, in principle, the difference with the modern experiments might not depend on the technological progress only but also on the different media that are tested thus preventing a straightforward comparison.

One should also take into account that, in the interpretation of the data, it was always assumed that any physical signal should only exhibit those smooth time modulations, associated with the earth rotation and its orbital revolution, which enter the motion of the laboratory with respect to a hypothetical preferred reference frame Σ, e.g. the Cosmic Microwave Background (CMB). The data instead were showing an irregular behavior indicating sizeably different directions of the drift at the same hour on consecutive days so that statistical averages were much smaller than all individual values. Within the traditional view, this has always represented a strong argument to interpret the measurements as mere instrumental artifacts.

Here, however, there might be a logical gap. The relation between the macroscopic earth motion and the microscopic propagation of light in a laboratory depends on a complicated chain of effects and, ultimately, on the physical nature of the vacuum. By comparing with the motion of a body in a fluid, the standard view corresponds to a form of regular, laminar flow where global and local velocity fields coincide. Instead, some arguments (see e.g. [1–3]), suggest that, at some fundamental level, the physical vacuum might resemble a turbulent fluid where large-scale and small-scale motions are only *indirectly* related. In this case, the parameters of the macroscopic Earth's motion would only fix the limiting boundaries for a microscopic velocity field which has an intrinsic non-deterministic nature.

The simplest explanation for this analogy is the intuitive representation of the vacuum as a fluid with vanishing viscosity. Then, in the framework of the Navier-Stokes equation, a laminar flow is by no means obvious due to the subtlety of the zero-viscosity (or infinite Reynolds number) limit, see for instance the discussion given by Feynman in Sect. 41.5, Vol.II of his Lectures [4]. The reason is that the velocity field of such a hypothetical fluid cannot be a differentiable function [5] and one should think, instead, in terms of continuous, nowhere differentiable functions, similar to ideal Brownian paths [6]. This gives

the idea of the vacuum as a fundamental stochastic medium consistently with some basic foundational aspects of *both* quantum physics and relativity .

In this different perspective, with forms of turbulence which, as in most models, become statistically isotropic at small scales, the direction of the local drift is a completely random quantity that has no definite limit by combining a large number of observations. Thus, one should first analyze the data in phase and amplitude (which give respectively the instantaneous direction and magnitude of the drift) and then concentrate on the latter which is a positive-definite quantity and remains non-zero under any averaging procedure. In this alternative picture, a non-vanishing amplitude (i.e. definitely larger than the experimental resolution) is the signature to separate an irregular, but genuine, signal from instrumental noise.

In this perspective, numerical simulations, as those performed in ref.[3], become essential. These calculations, confirming the first indications of ref.[15], indicate that in present ether-drift experiments with vacuum optical resonators [16–20], it is highly non trivial to understand if the observed irregular signal is just spurious noise or has a genuine physical origin. The reason is that, in the very high vacuum adopted in the experiments, the velocity of light becomes extremely close to the basic parameter c of Lorentz transformations where any observable effect is expected to vanish exactly. Therefore, one should run experiments slightly "off vacuum", where the refractive index $\mathcal{N} \neq 1$ but one can still control the analysis with the constraints posed by the absence of any measurable effect in the ideal $\mathcal{N} \to 1$ limit.

With this premise, light propagation in a gas of refractive index $\mathcal{N} = 1 + \epsilon$ was considered in detail (see the Appendix 2 of ref.[21]). In principle, (the solid container of) the gas can be at rest in Σ (case 1) or in the laboratory frame S' (case 2). For case 1, and for the Σ observer, it is customary to assume the isotropic metric $\gamma^{\mu\nu} = \mathrm{diag}(\mathcal{N}^2, -1, -1, -1)$. For case 2, on the other hand, the choice is not so obvious. To see why, let us denote by $g^{\mu\nu}$ the effective space-time metric for the S' observer and introduce the transformation matrix,

---

This picture was first proposed in the old ether theory at the end of XIX Century [7]. In this original derivation, the Lorentz covariance of Maxwell equations was not postulated from scratch but was emerging from an underlying physical system whose constituents obey classical mechanics. More recently, the turbulent-ether model has been re-formulated by Troshkin [8] (see also [9] and [10]) in the framework of the Navier-Stokes equation and by Saul [11] by starting from Boltzmann's transport equation. As another example, the same picture of the physical vacuum (or ether) as a turbulent fluid was Nelson's [12] starting point. In particular, the zero-viscosity limit gave him the motivation to expect that "the Brownian motion in the ether will not be smooth" and, therefore, to conceive the particular form of kinematics which is at the base of his stochastic derivation of the Schrödinger equation. A qualitatively similar picture is also obtained by representing relativistic particle propagation from the superposition, at very short time scales, of non-relativistic particle paths with different Newtonian mass [13] . In this formulation, particles randomly propagate (in the sense of Brownian motion) in an underlying granular medium which replaces the trivial empty vacuum [14] . For more details, see [3] .

say $A^{\mu}{}_{\nu}$, which for $\mathcal{N}=1$ connects the two metrics, i.e.

$$g^{\mu\nu} = A^{\mu}{}_{\sigma} A^{\nu}{}_{\rho} \gamma^{\sigma\rho} \tag{1}$$

The subtlety is that $A^{\mu}{}_{\nu}$ is a two-valued function for $\mathcal{N}=1$. In fact, when $\gamma^{\mu\nu}$ coincides with the Minkowski tensor $\eta^{\mu\nu} = \mathrm{diag}(1,-1,-1,-1)$, the standard choice to preserve the invariance of the velocity of light and get $g^{\mu\nu} = \eta^{\mu\nu}$ is $A^{\mu}{}_{\nu} = \Lambda^{\mu}_{\nu}$, where Λ^{μ}_{ν} is the Lorentz transformation matrix associated with the S' velocity v with respect to Σ. On the other hand for $\mathcal{N} \neq 1$, according to special relativity, to preserve isotropy and thus the equivalence of the two frames, one should instead fix $A^{\mu}{}_{\nu} = \delta^{\mu}{}_{\nu}$, this being the only way to get $g^{\mu\nu} = \gamma^{\mu\nu}$. But, for any finite v, Λ^{μ}_{ν} and $\delta^{\mu}{}_{\nu}$ cannot be related by a point transformation, thus, by continuity and in an infinitesimal region $\mathcal{N} = 1+\epsilon$, there are *two* solutions. Namely, if A^{μ}_{ν} is the identity matrix, we expect a first solution

$$[g^{\mu\nu}(\mathcal{N})]_1 = \gamma^{\mu\nu} \sim \eta^{\mu\nu} + 2\epsilon\ \delta^{\mu}_0 \delta^{\nu}_0 \tag{2}$$

while, if A^{μ}_{ν} is a Lorentz transformation, we expect the other solution

$$[g^{\mu\nu}(\mathcal{N})]_2 = \Lambda^{\mu}_{\rho} \Lambda^{\nu}_{\sigma} \gamma^{\rho\sigma} \sim \eta^{\mu\nu} + 2\epsilon\ v^{\mu} v^{\nu} \tag{3}$$

v^{μ} being the dimensionless S' 4-velocity, $v^{\mu} \equiv (v^0, \mathbf{v}/c)$ with $v_{\mu} v^{\mu} = 1$.

When combined with the idea of a stochastic vacuum, this leads to the effective metric for light propagation

$$\hat{g}^{\mu\nu}(t) \sim \eta^{\mu\nu} + 2\epsilon\ \hat{v}^{\mu}(t) \hat{v}^{\nu}(t) \tag{4}$$

where $\hat{v}^{\mu}(t)$ is a random velocity field which fluctuates around the average earth motion. In this new scheme, see ref.[22], the small irregular residuals observed in the classical experiments where light was still propagating in gaseous systems acquire a crucial importance and can become consistent with the average Earth's velocity of 370 km/s which is obtained from astronomical observations of the CMB. This surprising agreement motivates additional, precise checks with a new generation of laser interferometers where optical cavities are filled with a gaseous medium. The main aspects of this research will be summarized in the following.

2 Basic formalism

To illustrate the general framework, let us assume Eq.(3). As shown in ref.[21] (see Appendix 2), one can then solve the equation $g^{\mu\nu} p_{\mu} p_{\nu} = 0$ for light propagation and define the velocity of light $c_{\gamma}(\theta)$ from the ratio $p_0/|\mathbf{p}|$ where θ is the angle between $\mathbf{v}$ and $\mathbf{p}$ in the S' laboratory frame. Thus, one can compute the two way-velocity

$$\bar{c}_{\gamma}(\theta) = \frac{2\ c_{\gamma}(\theta) c_{\gamma}(\pi+\theta)}{c_{\gamma}(\theta) + c_{\gamma}(\pi+\theta)} \tag{5}$$

which gives

$$\bar{c}_{\gamma}(\theta) \sim \frac{c}{\mathcal{N}} \left[1 - \epsilon \frac{v^2}{c^2} \left(1 + \cos^2\theta \right) \right] \tag{6}$$

and a fractional light anisotropy

$$\frac{\Delta\bar{c}_\theta}{c} = \frac{\bar{c}_\gamma(\pi/2+\theta) - \bar{c}_\gamma(\theta)}{c} \sim \epsilon\, \frac{v^2}{c^2} \cos 2(\theta - \theta_0) \tag{7}$$

Here, the pair (v, θ_0) describes the magnitude and the direction of the local drift in the relevant plane of the interferometer. Then, from the basic relations of modern ether-drift experiments [16], this is directly related to the frequency shift between two orthogonal optical resonators

$$\frac{\Delta\bar{c}_\theta}{c} \sim \frac{\Delta\nu(\theta)}{\nu_0} \tag{8}$$

Likewise, one can compare with the fringe patterns measured in the classical Michelson-Morley experiments. These depend on the time difference $\Delta t(\theta)$ for light propagation back and forth along perpendicular paths of length L

$$\Delta t(\theta) = \frac{2L}{\bar{c}_\gamma(\theta)} - \frac{2L}{\bar{c}_\gamma(\pi/2+\theta)} \sim \frac{2L}{c}\, \frac{\Delta\bar{c}_\theta}{c} \tag{9}$$

(where, in the last relation, we have assumed that light propagates in a medium of refractive index $\mathcal{N} = 1+\epsilon$, with $\epsilon \ll 1$). This gives directly the fringe patterns (λ is the light wavelength)

$$\frac{\Delta\lambda(\theta)}{\lambda} \sim \frac{2L}{\lambda}\, \frac{\Delta\bar{c}_\theta}{c} \tag{10}$$

Thus both the frequency shifts of the modern experiments and the fringe shifts of the classical experiments depend on the light anisotropy

$$\frac{\Delta\bar{c}_\theta(t)}{c} = 2S(t)\sin 2\theta + 2C(t)\cos 2\theta \tag{11}$$

where

$$C(t) = \frac{1}{2}\epsilon\, \frac{v_x^2(t) - v_y^2(t)}{c^2} \qquad\qquad S(t) = \frac{1}{2}\epsilon\, \frac{2v_x(t)v_y(t)}{c^2} \tag{12}$$

with $v_x(t) = v(t)\cos\theta_0(t)$, $v_y(t) = v(t)\sin\theta_0(t)$ and we have made explicit the time dependence of the signal.

As anticipated, the standard analysis of the data has been based on the idea of smooth, regular modulations of the signal associated with a cosmic earth velocity. In general, this is characterized by a magnitude V, a right ascension α and an angular declination γ. These parameters can be considered constant for short-time observations of a few days where there are no appreciable changes due to the earth orbital velocity around the sun. In this framework, where the only time dependence is due to the earth rotation, the traditional identifications are $v_x(t) \equiv \tilde{v}_x(t)$ and $v_y(t) \equiv \tilde{v}_y(t)$ as from the simple application of spherical trigonometry [23]

$$\cos z(t) = \sin\gamma\sin\phi + \cos\gamma\cos\phi\cos(\tau - \alpha) \tag{13}$$

$$\tilde{v}(t) = V\sin z(t) \tag{14}$$

$$\tilde{v}_x(t) = \tilde{v}(t)\cos\tilde{\theta}_0(t) = V\left[\sin\gamma\cos\phi - \cos\gamma\sin\phi\cos(\tau-\alpha)\right] \tag{15}$$

$$\tilde{v}_y(t) = \tilde{v}(t)\sin\tilde{\theta}_0(t) = V\cos\gamma\sin(\tau-\alpha) \tag{16}$$

Here $z = z(t)$ is the zenithal distance of $\mathbf{V}$, ϕ is the latitude of the laboratory, $\tau = \omega_{\rm sid}t$ is the sidereal time of the observation in degrees ($\omega_{\rm sid} \sim \frac{2\pi}{23^h 56'}$) and the angle θ_0 is counted conventionally from North through East so that North is $\theta_0 = 0$ and East is $\theta_0 = 90^o$. With the identifications $v_x(t) \equiv \tilde{v}_x(t)$ and $v_y(t) \equiv \tilde{v}_y(t)$, one thus arrives to the simple Fourier decomposition

$$S(t) \equiv \tilde{S}(t) = S_0 + S_{s1}\sin\tau + S_{c1}\cos\tau + S_{s2}\sin(2\tau) + S_{c2}\cos(2\tau) \tag{17}$$

$$C(t) \equiv \tilde{C}(t) = C_0 + C_{s1}\sin\tau + C_{c1}\cos\tau + C_{s2}\sin(2\tau) + C_{c2}\cos(2\tau) \tag{18}$$

with *time-independent* C_k and S_k Fourier coefficients.

On the other hand, let us assume that the vacuum behaves as a stochastic medium similar to a turbulent fluid. Then, the parameters of the macroscopic Earth's motion would not directly determine the local flow but just fix the typical limiting boundaries for a microscopic velocity field which has an intrinsic non deterministic nature. This means that Eqs.(17,18) are no longer valid and one should instead go back to Eq.(12) by identifying $v_x(t) = \hat{v}_x(t)$ and $v_y(t) = \hat{v}_y(t)$ with a random velocity field as in Eq.(4). By following ref.[24], in the limit of homogeneous turbulence, these velocity components can then be generated by the method of unsteady random Fourier series.

The perspective is that of an observer moving in the turbulent fluid who wants to describe the two velocity components in his x-y plane at a fixed location in his laboratory. For homogeneous turbulence, one finds the general expressions

$$\hat{v}_x(t) = \sum_{n=1}^{\infty}\left[x_n(1)\cos\omega_n t + x_n(2)\sin\omega_n t\right] \tag{19}$$

$$\hat{v}_y(t) = \sum_{n=1}^{\infty}\left[y_n(1)\cos\omega_n t + y_n(2)\sin\omega_n t\right] \tag{20}$$

where $\omega_n = 2n\pi/T$, T being a time scale which represents a common period of all stochastic components. The coefficients $x_n(i=1,2)$ and $y_n(i=1,2)$ are random variables with zero mean and have the physical dimension of a velocity. Here the macroscopic Earth's motion enters: to determine their limiting boundaries. To this end, let us denote by $[-d_x(t), d_x(t)]$ the range for $x_n(i=1,2)$ and by $[-d_y(t), d_y(t)]$ as the corresponding range for $y_n(i=1,2)$. In terms of these boundaries, the only non-vanishing (quadratic) statistical averages are

$$\langle x_n^2(i=1,2)\rangle_{\rm stat} = \frac{d_x^2(t)}{3\ n^{2\eta}} \qquad\qquad \langle y_n^2(i=1,2)\rangle_{\rm stat} = \frac{d_y^2(t)}{3\ n^{2\eta}} \tag{21}$$

in a uniform probability model within the intervals $[-d_x(t), d_x(t)]$ and $[-d_y(t), d_y(t)]$. Here, the exponent η controls the power spectrum of the fluctuating components. For numerical simulations, between the two values $\eta = 5/6$ and $\eta = 1$ reported in ref.[24], one should fix $\eta = 1$ which corresponds to the point of view of an observer moving in the fluid. Finally, these boundaries can be determined

from the kinematical parameters (V, α, γ) which describe the macroscopic earth motion with the identifications $d_x(t) = \tilde{v}_x(t)$ and $d_y(t) = \tilde{v}_y(t)$ as in Eqs.(13)-(16). For numerical simulations, the parameters were fixed to their average values obtained from the CMB observations, i.e. $V \sim 370$ km/s, $\alpha \sim 168$ degrees, $\gamma \sim$ - 6 degrees. If, however, we impose statistical isotropy, the relation

$$\tilde{v}_x^2(t) + \tilde{v}_y^2(t) = \tilde{v}^2(t) \tag{22}$$

requires the identification

$$d_x(t) = d_y(t) = \frac{\tilde{v}(t)}{\sqrt{2}} \tag{23}$$

For such isotropic model, by combining Eqs.(19)−(23) and in the limit of an infinite statistics, one gets

$$\langle \hat{v}_x^2(t) \rangle_{\rm stat} = \langle \hat{v}_y^2(t) \rangle_{\rm stat} = \frac{\tilde{v}^2(t)}{2} \ \frac{1}{3} \sum_{n=1}^{\infty} \frac{1}{n^2} = \frac{\tilde{v}^2(t)}{2} \ \frac{\pi^2}{18}$$
$$\langle \hat{v}_x(t) \hat{v}_y(t) \rangle_{\rm stat} = 0 \tag{24}$$

and vanishing statistical averages

$$\langle C(t) \rangle_{\rm stat} = 0 \qquad\qquad \langle S(t) \rangle_{\rm stat} = 0 \tag{25}$$

at *any* time t, see Eqs.(12). Therefore, by construction, this model gives a definite non-zero signal but, if the same signal were fitted with Eqs.(17) and (18), it also gives average values $(C_k)^{\rm avg} = 0$, $(S_k)^{\rm avg} = 0$ for the Fourier coefficients.

3 Comparison with the classical ether-drift experiments

In the absence of experiments where optical resonators are filled by gaseous media, a detailed comparison [22] was performed with the fringe patterns measured in the classical ether-drift experiments. To fully appreciate the change of perspective implied by Eqs.(25), let us consider the traditional procedure of data taking in the classical experiments. Fringe shifts were observed at the same sidereal time on a few consecutive days (so that changes in the earth orbital velocity could be ignored) and the data were averaged at any given angle θ. In this way, by combining Eqs.(10) and (11), one was obtaining

$$\langle \frac{\Delta\lambda(\theta; t)}{\lambda} \rangle_{\rm stat} = \frac{2L}{\lambda} \left[2 \sin 2\theta \ \langle S(t) \rangle_{\rm stat} + 2 \cos 2\theta \ \langle C(t) \rangle_{\rm stat} \right] \tag{26}$$

and these averages were compared with various models of cosmic motion.

But, if the ether-drift is a genuine stochastic phenomenon, as expected if the physical vacuum were similar to a turbulent fluid which becomes isotropic at small scales, these average combinations should vanish *exactly* for an infinite number of measurements. Thus, averages of vectorial quantities are non vanishing just because the statistics is finite and forming the averages Eq.(26) is

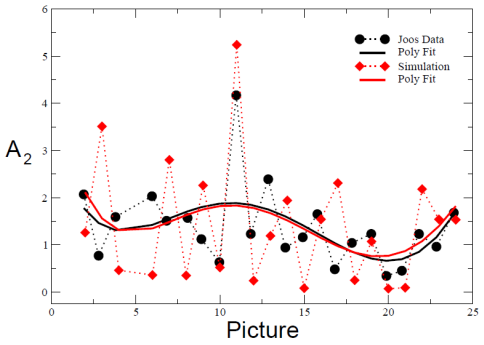

Fig. 1. Joos' experimental amplitudes in units 10^{-3} are compared with a single simulation of 22 measurements performed at Joos times. The stochastic velocity components are controlled by the kinematical parameters $(V, \alpha, \gamma)_{\rm CMB}$. By changing the parameters of the simulation, the typical variation of each simulated entry is $(1 \div 4) \cdot 10^{-3}$ depending on the sidereal time. We also show two 5th-order polynomial fits to the two different sets of values. The figure is taken from ref.[22] .

not a meaningful procedure. In particular, the direction $\theta_0(t)$ of the drift in the plane of the interferometer (defined by the relation $\tan 2\theta_0(t) = S(t)/C(t)$) is a completely random quantity which has no definite limit by combining a large number of observations. Instead, one should separate the signal in phase and amplitude (which give respectively the instantaneous direction and magnitude of the local drift) and concentrate on the latter which is a positive-definite quantity and remains non-zero under any averaging procedure.

To this end, from Eqs.(12) we find

$$\frac{\Delta\lambda(t,\theta)}{\lambda} \sim \frac{L}{\lambda}\,\frac{2\epsilon\; v^2(t)}{c^2}\cos 2[\theta - \theta_0(t)] \equiv A_2(t)\cos 2[\theta - \theta_0(t)] \qquad (27)$$

In this way, the 2nd-harmonic amplitude $A_2(t)$ depends on an *observable* velocity

$$v^2_{\rm obs}(t) \sim 2\epsilon\; v^2(t) \qquad (28)$$

which is re-scaled by the tiny factor 2ϵ with respect to the *kinematical* velocity v^2 which instead enters the classical prediction

$$\left[\frac{\Delta\lambda(t,\theta)}{\lambda}\right]_{\rm class} \sim \frac{L}{\lambda}\,\frac{v^2(t)}{c^2}\cos 2[\theta - \theta_0(t)] \equiv A_2^{\rm class}(t)\cos 2[\theta - \theta_0(t)] \qquad (29)$$

Therefore, the differences with respect to the traditional analysis are: a) the re-scaling $v(t) \to v_{\rm obs}(t)$ and b) the inclusion of the random variations of the velocity field mentioned above with the identifications $v_x(t) = \hat{v}_x(t)$ and $v_y(t) = \hat{v}_y(t)$ as in Eqs.(19) and (20).

By implementing these two ingredients, things change completely. To have an idea, we report in Figs. 1 and 2 the comparison between numerical simulations and the experimental second harmonic amplitudes extracted from the

most precise classical ether-drift experiment, the one performed by Joos in 1930 [25].

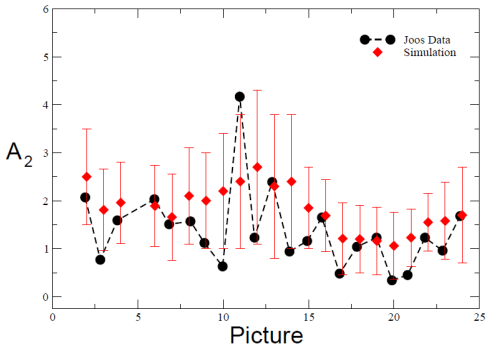

Fig. 2. Joos' experimental amplitudes in units 10^{-3} are compared with the result of simulating the averaging process over 10 hypothetical measurements performed, at each Joos' time, on 10 consecutive days. The stochastic velocity components are controlled by the kinematical parameters $(V, \alpha, \gamma)_{\rm CMB}$. The effect of varying the parameters of the simulation has been approximated into a central value and a symmetric error. The figure is taken from ref.[22] .

The analysis of ref.[22] is summarized in Table 1 where we have also included the determinations from the Tomaschek [26] and Piccard-Stahel experiments [27]. The refractivities used in Eq.(28), to transform observable velocity into kinematical velocity, were $\epsilon = 2.8 \cdot 10^{-4}$ and $\epsilon = 3.3 \cdot 10^{-5}$ as respectively for air and gaseous helium at room temperature and atmospheric pressure.

The only possible discrepancy found in ref.[22] concerned the Michelson-Pease-Pearson (MPP) experiment at Mount Wilson which was giving a considerably smaller central value, namely $v \sim 180$ km/s, for the kinematical velocity, even though the associated uncertainty could not be estimated. However, we will now show that, within statistical uncertainties, also the MPP experiment can become consistent with our stochastic model.

As discussed in [22] it is extremely difficult to understand the results of the MPP experiment from the original articles [28,29]. No numerical results are reported and the two papers are even in contradiction about the magnitude of the measured effects ("one-fifteenth" of the expected value vs. "one-fiftieth"). To try to understand, we have consulted another article which, rather surprisingly, was signed by Pease alone [30]. In this article, Pease declares that, in

---

The velocities for the Piccard-Stahel experiment [27] derive from the value $L/\lambda = 6.4 \cdot 10^6$ and the average 2nd-harmonic amplitude $(2.8 \pm 1.5) \cdot 10^{-3}$. This is obtained from their individual 24 determinations namely (in units 10^{-3}), the 12 Mt.Rigi values $A_2^{\rm EXP} = 3.4,\ 1.1,\ 4.0,\ 2.4,\ 2.4,\ 4.3,\ 2.3,\ 2.6,\ 0.6,\ 2.0,\ 1.2,\ 3.9$, and the 12 Brussels measurements, at night $A_2^{\rm EXP} = 3.2,\ 5.2,\ 6.5,\ 2.2,\ 4.9,\ 3.8$ and in the morning $A_2^{\rm EXP} = 1.85,\ 1.27,\ 3.40,\ 1.00,\ 3.70,\ 1.14$.

Table 1. *The average velocity observed (or the limits placed) by the classical ether-drift experiments in the alternative interpretation where the relation between the observable $v_{\rm obs}$ and the kinematical v is governed by Eq.(28).*

Experiment	gas in the interferometer	$v_{\rm obs}$(km/s)	v(km/s)
Michelson-Morley(1887)	air	$8.4^{+1.5}_{-1.7}$	355^{+62}_{-70}
Morley-Miller(1902-1905)	air	8.5 ± 1.5	359 ± 62
Miller(1925-1926)	air	$8.4^{+1.9}_{-2.5}$	355^{+79}_{-104}
Tomaschek (1924)	air	$7.7^{+2.1}_{-2.8}$	325^{+87}_{-116}
Kennedy(1926)	helium	< 5	< 600
Illingworth(1927)	helium	$2.4^{+0.8}_{-1.2}$	295^{+98}_{-146}
Piccard-Stahel(1926-1927)	air	$6.3^{+1.5}_{-2.0}$	266^{+62}_{-83}
Michelson-Pease-Pearson(1929)	air	$4.3 \pm ...$	$182 \pm ...$
Joos(1930)	helium	$1.8^{+0.5}_{-0.6}$	226^{+63}_{-76}

their experiment, to test Miller's claims, they concentrated on a purely *differential* type of measurement. For this reason, he only reports the quantity

$$\delta(\theta) = \langle \frac{\Delta\lambda(\theta; t = 5:30)}{\lambda} \rangle_{\rm stat} - \langle \frac{\Delta\lambda(\theta; t = 17:30)}{\lambda} \rangle_{\rm stat}$$

This means that they were performing a large set of observations at sidereal time 5:30 and averaging the data. Then, the same procedure was carried out, in the same days, at sidereal time 17:30. Finally, the two averages were subtracted to form the quantities $\delta(\theta)$. These are typically below ± 0.004 and this is the order of magnitude which is usually compared [31] with the classical expectation for the MPP apparatus, namely $A_2^{\rm class} = \frac{L}{\lambda} \frac{(30{\rm km/s})^2}{c^2} \sim 0.45$ for optical path of 85 feet or $A_2^{\rm class} = \frac{L}{\lambda} \frac{(30{\rm km/s})^2}{c^2} \sim 0.29$ for optical path of 55 feet.

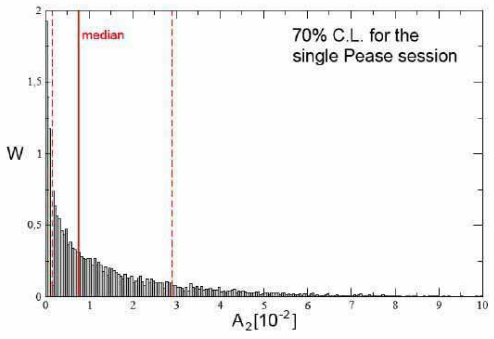

Fig. 3. The histogram W of a numerical simulation of 10.000 instantaneous amplitudes for the single session of January 13, 1928, reported by Pease [30]. The vertical normalization is to a unit area. We show the median and the 70% CL. The limits on the random Fourier components in Eqs.(19) and (20) were fixed by the CMB kinematical parameters as explained in the text.

As explained above, by accepting a stochastic picture of the ether-drift, the vector average of more and more observations will wash out completely the physical information contained in the original measurements. Therefore, from these $\delta-$values, nothing can be said about the magnitude of the fringe shifts $\frac{\Delta\lambda(\theta)}{\lambda}$ obtained in the individual measurements, i.e. before any averaging procedure and before any subtraction. Pease just reports a poor-quality plot of a single observation, performed on January 13, 1928, when the length of the optical path was still 55 feet. In this plot, the fringes vary approximately in the range ± 0.006 whose absolute value may be taken to estimate the amplitude of that observation.

We have thus performed a numerical simulation in our stochastic model by generating 10,000 values of the amplitude, at the same sidereal time 5:30 of the observation reported by Pease, and using the CMB kinematical parameters to bound the random Fourier components of the velocity field Eqs.(19) and (20). The resulting histogram, reported in Fig.3, shows that the value $A_2 \sim 0.006$ lies well within the 70% Confidence Limit. Notice the large probability content at very small amplitudes and the long tail extending up to $A_2 = 0.030$ or even larger values.

The wide interval of amplitudes corresponding to the 70% C. L. (which could be expressed as $0.014^{+0.015}_{-0.012}$) indicates that, in our stochastic model, one could accomodate individual MPP observations with an amplitude as 0.002 or as 0.030 which is fifteen times larger. This is another crucial difference with a deterministic model of the ether-drift. In this traditional view, in fact, the amplitude can vary at most by a factor $r = (v_{\max}/v_{\min})^2$ where $v_{\max}$ and $v_{\min}$ are respectively the maximum and minimum daily projection of the earth velocity in the interferometer plane. Therefore, since r varies typically by a factor of two, the observation of such large fluctuations in the data would induce to conclude, in a deterministic model, that there must be some systematic effect which modifies the measurements in an uncontrolled way.

4 Conclusions

The overall consistency of our picture with the classical experiments should induce to perform the new dedicated experiments where the optical resonators which are coupled to the lasers (see Fig.4) are filled by gaseous media. In this case,one should check the relative frequency shift in Eq.(8) and study the substantially larger frequency shift which should be observed with respect to the present experiments with vacuum optical cavities.

These experiments will likely require a good deal of ingenuity and technical skill. For instance, an important element to increase the overall stability and minimize systematic effects may consist in obtaining the two optical resonators

Strictly speaking, for a more precise comparison with the data, one should fold the histogram with a smearing function which takes into account the finite resolution Δ of the apparatus. The resulting curve will bend for $A_2 \to 0$ and saturate to a limit which depends on Δ. Nevertheless, this refinement should not modify substantially the probability content around the median which is very close to $A_2 = 0.007$.

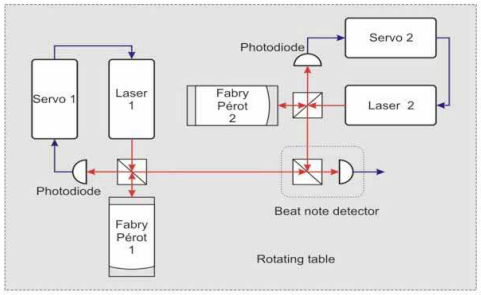

Fig. 4. The scheme of a modern ether-drift experiment. The light frequencies are first stabilized by coupling the lasers to Fabry-Perot optical resonators. The frequencies ν_1 and ν_2 of the signals from the resonators are then compared in the beat note detector which provides the frequency shift $\Delta\nu = \nu_1 - \nu_2$. In present experiments a very high vacuum is maintained within the resonators.

from the same block of material as with the crossed optical cavity of ref.[32]. Still, measuring precisely the frequency shift in the gas mode will be a delicate issue. To fix the ideas, let us consider gaseous helium at atmospheric pressure, a velocity $v = 300$ km/s and a typical laser frequency of about $3 \cdot 10^{14}$ Hz. In these conditions, the expected shift is $\Delta\nu \sim 10$ kHz. This is much smaller than many effects which must preliminarily be subtracted. For instance, by changing from vacuum to the gas case under pressure, and for a typical cavity length of 10 cm, the effect of cavity deformations is about 10 MHz [33]. Theoretically, this should not depend on the gas used but only on the solid parts of the apparatus. Yet, experimental measurements at atmospheric pressure show that there is a difference between Nitrogen and Helium of about 0.6 MHz [33]. Therefore, one should lower the pressure to reduce this spurious effect. Of course, this is what might show up in a single cavity while we are interested in the frequency shift between two cavities where the effect will be reduced. Nevertheless, the pressure will have to be lowered and, then, also the signal will be reduced correspondingly. Therefore, several technical problems must be solved before concluding that, in the gas case, there is a definite improvement with respect to the classical experiments (in particular with respect to Joos).

This substantial enhancement is confirmed by the only modern experiment performed in similar conditions: the 1963 MIT experiment by Jaseja et. al [34] . Actually, at that time, they did not use optical resonators but were comparing directly the frequencies of two He-Ne lasers under 90 degrees rotations of the apparatus. However, the light from the lasers emerges from a He-Ne gas mixture and thus the two laser frequencies represent a measure of the two-way velocity of light, along orthogonal directions, in that environment. Finally, for a proper comparison, one has to subtract preliminarily a large systematic constant shift of about 270 kHz interpreted as being due to magnetostriction in the Invar spacers induced by the Earth's magnetic field. As suggested by the same authors, this spurious effect, that was only affecting the overall normalization

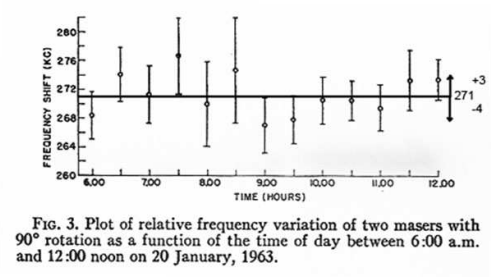

FIG. 3. Plot of relative frequency variation of two masers with 90° rotation as a function of the time of day between 6:00 a.m. and 12:00 noon on 20 January, 1963.

Fig. 5. The data of ref.[34] for the frequency shift between two He-Ne masers. The double arrow indicates the range of variation in the same model Eq.(8) used for the classical experiments.

of the experimental $\Delta\nu$, can be subtracted by looking at the time variations of the data.

Now assuming a preferred frame, the shift is maximal for 90 degree rotations with respect to the true direction of the earth motion. This means a frequency shift

$$\text{Shift} \lesssim |\Delta\nu(\theta = 0) - \Delta\nu(\theta = \pi/2)| \sim 2(\mathcal{N}_{\text{He-Ne}} - 1)\ (v^2/c^2)\ \nu_0 \qquad (30)$$

Then for a laser frequency $\nu_0 \sim 2.6 \cdot 10^{14}$ Hz, a refractive index $\mathcal{N}_{\text{He-Ne}} \sim 1.00004$ and a cosmic earth velocity of about 315^{+20}_{-25} km/s (as for the earth cosmic motion at the latitude of Boston and at the time of the observations) the expected frequency shift would be [35]

$$\text{Shift} \lesssim 23.6\ ^{+3.1}_{-4.2}\ \text{kHz} \qquad (31)$$

Therefore, once the mean value of 23.6 kHz is hidden in the much larger spurious shift of 270 kHz, we would expect typical relative variations of about $+3$ and -4 kHz (respectively above and below the mean value). This expectation is roughly consistent with residual variations of a few kHz shown in Fig.5. This fairly good agreement gives further motivations for the new series of experimental tests.

References

1. M. Consoli, A. Pluchino and A. Rapisarda, Chaos Solitons Fract **44**, 1089 (2011).
2. M. Consoli, Phys. Lett. **A376**, 3377 (2012).
3. M. Consoli, et al. Physica A **394**, 61 (2014).
4. R. P. Feynman, R. B. Leighton and M. Sands, The Feynman Lectures on Physics, Addison Wesley Publ. Co. 1963.
5. L. Onsager, Nuovo Cimento, Suppl. **6**, 279 (1949).
6. G. L. Eyink and K. R. Sreenivasan Rev. Mod. Phys. **78**, 87 (2006).
7. E. T. Whittaker, A History of the Theories of Aether and Electricity, Dover Publications, Inc. New York 1989.
8. O. V. Troshkin, Physica **A168**, 881-899 (1990).

9. H. E. Puthoff, Linearized turbulent flow as an analog model for linearized General Relativity, arXiv:0808.3401 [physics.gen-ph].
10. T. D. Tsankov, Classical Electrodynamics and the Turbulent Aether Hypothesis, Preprint February 2009, unpublished.
11. L. A. Saul, Phys. Lett. **A 314** (2003) 472.
12. E. Nelson, Phys. Rev. **150** (1966) 1079.
13. P. Jizba and H. Kleinert, Phys. Rev. **D82** (2010) 085016.
14. P. Jizba and F. Scardigli, Special Relativity induced by Granular Space, arXiV:1301.4091v2[hep-th].
15. M. Consoli and L. Pappalardo, Gen. Rel. and Grav. **42** (2010) 2585.
16. For a comprehensive review, see H. Müller et al., Appl. Phys. B **77**, 719 (2003).
17. S. Herrmann, et al., Phys.Rev. D **80**, 10511 (2009).
18. Ch. Eisele, A. Newsky and S. Schiller, Phys. Rev. Lett. **103**, 090401 (2009).
19. M. Nagel et al., Ultra-stable Cryogenic Optical Resonators For Tests Of Fundamental Physics, arXiv:1308.5582[physics.optics].
20. Q. Chen, E. Magoulakis, and S. Schiller,Phys. Rev. **D 93** , 022003 (2016).
21. M. Consoli, Found. of Phys. **45** (2015) 22.
22. M. Consoli, C. Matheson and A. Pluchino, Eur. Phys. J. Plus **128**, 71 (2013).
23. J. J. Nassau and P. M. Morse, Ap. J. **65**, 73 (1927).
24. J. C. H. Fung et al., J. Fluid Mech. **236**, 281 (1992).
25. G. Joos, Ann. d. Physik **7** (1930) 385.
26. R. Tomaschek, Astron. Nachrichten, **219** (1923) 301, English translation.
27. A. Piccard and E. Stahel, Journ. de Physique et Le Radium **IX** (1928) No.2.
28. A. A. Michelson, F. G. Pease and F. Pearson, Nature **123** (1929) 88.
29. A. A. Michelson, F. G. Pease and F. Pearson, J. Opt. Soc. Am. **18** (1929) 181.
30. F. G. Pease, Publ. of the Astr. Soc. of the Pacific, **XLII** (1930) 197.
31. R. S. Shankland et al., Rev. Mod. Phys.**27** (1955) 167.
32. Ch. Eisele et al., Opt. Comm. **281**, 1189 (2008).
33. J. A. Stone and A. Stejskal, Metrologia **41**, 189 (2004).
34. T. S. Jaseja, et al., Phys. Rev. **133**, A1221 (1964).
35. M. Consoli, A. Pluchino and A. Rapisarda, Europhysics Lett. **113**, 19001 (2016), also arXiv:1601.06518 [astro-ph.CO]RC, London, 2009.